Electronic Supplementary Material (ESI) for Environmental Science: Water Research & Technology.

Supporting Information

Understanding Fecal Sludge Drying in Membrane-Lined Container-Based Toilets for Developing Countries with CFD Modeling

Babak EbraziBakhshayesh[1] and Paul Imhoff[1*]

[1]Department of Civil and Environmental Engineering, University of Delaware, 344A DuPont Hall, Newark, DE

* Corresponding Author – Email: imhoff@udel.edu

1. Estimation of eVent laminate's properties

1.1. Estimation of porosity

The eVent laminate consists of an ePTFE membrane contained between an inner hydrophilic support fabric and an outer hydrophobic polyester fabric, where for the laminate-lined toilet the hydrophilic fabric is filled with liquid. The effective porosity of the eVent laminate for water vapor diffusion is a function of the effective porosity of the hydrophobic components, the ePTFE membrane and outer hydrophobic fabric, and was determined using

$$\varepsilon^l = \frac{\left(\rho^f \times \delta^f \times \varepsilon^f\right) + \left(\rho^m \times \delta^m \times \varepsilon^m\right)}{\left(\rho^f \times \delta^f\right) + \left(\rho^m \times \delta^m\right)} \qquad \text{S1}$$

where ε is dimensionless porosity, δ is thickness, ρ is density, and superscripts *f, m, and l* represent the hydrophobic fabric, membrane and laminate, respectively.

1.2. Estimation of thermal properties

The effective thermal conductivity for heat transport through the hydrophobic components of the eVent laminate was determined using

$$k_{eff}^f = \varepsilon^f k^g + (1 - \varepsilon^f) k^f \qquad \text{S2}$$

$$k_{eff}^m = \varepsilon^m k^g + (1 - \varepsilon^m) k^m \qquad \text{S3}$$

$$k^l = \frac{\delta^f + \delta^m}{\dfrac{\delta^f}{k_{eff}^f} + \dfrac{\delta^m}{k_{eff}^m}} \qquad \text{S4}$$

where k and k_{eff} are thermal conductivity and effective thermal conductivity, and superscripts *f*, *m,* and g represent hydrophobic fabric, membrane and gas domain, respectively. The hydrophobic fabric and membrane are assumed to be filled with gas. The specific heat capacity of the hydrophobic components of the eVent laminate was estimated using

$$c_p^l = \frac{\left(\rho^f \times \delta^f \times c_p^f\right) + \left(\rho^m \times \delta^m \times c_p^m\right)}{\left(\rho^f \times \delta^f\right) + \left(\rho^m \times \delta^m\right)} \qquad \text{S5}$$

where c_p is the effective specific heat capacity of the laminate. All parameters defined for the eVent laminate are listed in Table. S1.

2. Tables

Table S1. eVent laminate parameters

Parameter	Description	Value	Reference
c_p^f	Specific heat capacity of hydrophobic fabric	1150 J/kg K	Ref. [1]
c_p^l	Specific heat capacity of ePTFE membrane/hydrophobic fabric	1203 J/kg K	Estimated using equation S5
c_p^m	Specific heat capacity of ePTFE membrane	1300 J/kg K	Ref. [2]
k^f	Thermal conductivity of hydrophobic fabric	0.2 W/m °K	Ref. [1]
k_{eff}^f	Effective thermal conductivity of the air-filled hydrophobic fabric	0.1 W/m °K	Estimated using equation S2
k^g	Thermal conductivity of air	0.026 W/m °K	Ref. [3]
k^l	Effective thermal conductivity of ePTFE membrane/ hydrophobic fabric	0.09 W/m °K	Estimated using equation S4
k^m	Thermal conductivity of ePTFE membrane	0.3 W/m °K	Ref. [2]
k_{eff}^m	Effective thermal conductivity of the air-filled ePTFE membrane	0.07 W/m °K	Estimated using equation S3
δ^f	Thickness of the hydrophobic fabric	0.15 mm	Measured
δ^m	Thickness of the ePTFE membrane	0.05 mm	Measured
ε^f	Porosity of hydrophobic fabric	0.58	Ref. [4]
ε^l	Porosity of ePTFE membrane/ hydrophobic fabric	0.67	Estimated using equation S1
ε^m	Porosity of ePTFE membrane	0.84	Ref. [2]
ρ^f	Density of hydrophobic fabric	1345 kg / m3	Ref. [1]
ρ^m	Density of ePTFE membrane	2250 kg / m3	Ref. [2]

Table S2. Parameters of the eVent laminate used for simulating three drying replicate drying experiments

Parameter	**Value**
Laminate thickness (δ)	0.2 mm
Laminate porosity (ε^l)[a]	0.67
Laminate density (ρ^l)[a]	1571 kg / m3
Laminate thermal conductivity (k^l)[a]	0.1 (W/m ^{0}C)
Laminate heat capacity (C_p^l)[a]	1.2 (kJ/kg ^{0}C)

[a] Estimated for the hydrophobic components of the laminate: ePTFE membrane and hydrophobic fabric.

Table S3. Initial conditions used for laminate jar, box and laminated-lined 40 L drum drying simulation conducted in controlled conditions

Setup	**Water vapor concentration in gas and laminate domains (mol/m^3)**	**Temperature in all domains (° C)**
Laminate jar	0.56	31.4
Laminate box	0.43	28.93
Laminated-lined 40 L drum	0.38	28.03

Table S4. Boundary conditions used in laminate jar drying simulation

Location	**Momentum transfer**	**Mass transfer**	**Heat transfer**
Air inlet	u^g= 0.40 m/s	C_w^g = 0.56 mol/m^3	T^g= 31.4 ° C
Air outlet	$P^g = P_{atm}$	$-\vec{n}.[D_w^g \nabla C_w^g] = 0$	$-\vec{n}.[-K^g \nabla T^g] = 0$
Jar wall (gas domain)	u^g= 0	$-\vec{n}.[-D_w^g \nabla C_w^g + \vec{u}^g \nabla C$ $] = 0$	$T_{wall} = T^g$
Jar wall (aqueous domain)	NA	NA	$T_{wall} = T^a$
Gas & laminate domain interface	u^g= 0	$C_w^l = C_w^g$	$T^l = T^g$
Aqueous & laminate domain interface	NA	$C_w^l = C_w^{g*}$	$T^l = T^a$
Aqueous & headspace domain interface	NA	$C_w^g = C_w^{g*}$	$T^g = T^a$
Symmetry plane	$\frac{\partial u_y^g}{\partial y} = 0$	$\frac{\partial C_w^g}{\partial y} = \frac{\partial C_w^l}{\partial y} = 0$	$\frac{\partial T^l}{\partial y} = \frac{\partial T^a}{\partial y} = \frac{\partial T^g}{\partial y} = 0$

Table S5. Boundary conditions used in drying simulation of the laminate box

Location	**Momentum transfer**	**Mass transfer**	**Heat transfer**
Air inlet	u^g= 0.17 m/s	C_w^g = 0.43 mol/m^3	T^g = 28.93° C
Air outlet	$P^g = P_{atm}$	$-\vec{n}.[D_w^g \nabla C_w^g] = 0$	$-\vec{n}.[-K^g \nabla T^g] = 0$
Gas & laminate domain interface	u^g= 0	$C_w^l = C_w^g$	$T^l = T^g$
Aqueous & laminate domain interface	NA	$C_w^l = C_w^{g*}$	$T^l = T^a$
Aqueous & domain interface	NA	$C_w^g = C_w^{g*}$	$T^g = T^a$
Symmetry plane	$\frac{\partial u_y^g}{\partial y} = 0$	$\frac{\partial C_w^g}{\partial y} = \frac{\partial C_w^l}{\partial y} = 0$	$\frac{\partial T^l}{\partial y} = \frac{\partial T^a}{\partial y} = \frac{\partial T^g}{\partial y} = 0$

Table S6. Boundary conditions used for laminated-lined 40 L drum drying simulation under controlled conditions.

Location	**Momentum transfer**	**Mass transfer**	**Heat transfer**
Air inlet	$u^g = 0.13$ m/s	$C_w^g = 0.38$ mol/m^3	$T^g = 28.03$ ° C
Air outlet	$P^g = P_{atm}$	$-\vec{n}.\left[D_w^g \nabla C_w^g\right] = 0$	$-\vec{n}.[-K^g \nabla T^g] = 0$
Drum wall (gas domain)	$u^g = 0$	$-\vec{n}.[-D_w^g \nabla C_w^g + \vec{u}^g \nabla C_w^g] = 0$	$T_{wall} = T^g$
Gas & laminate domain interface	$\vec{u}^g = 0$	$C_w^l = C_w^g$	$T^l = T^g$
Aqueous & laminate domain interface	NA	$C_w^l = C_w^{g*}$	$T^l = T^a$
Aqueous & headspace domain interface	NA	$C_w^g = C_w^{g*}$	$T^g = T^a$
Symmetry plane	$\frac{\partial u_y^g}{\partial y} = 0$	$\frac{\partial C_w^g}{\partial y} = \frac{\partial C_w^l}{\partial y} = 0$	$\frac{\partial T^l}{\partial y} = \frac{\partial T^a}{\partial y} = \frac{\partial T^g}{\partial y} = 0$

3. Figures

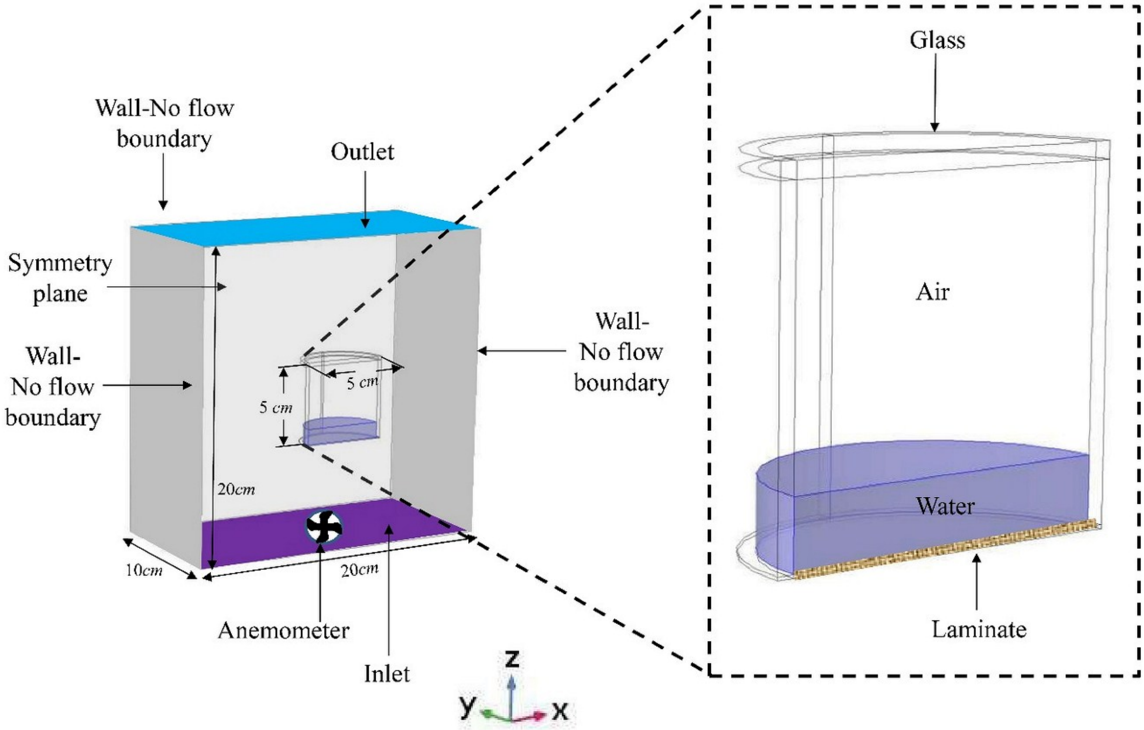

Fig. S1. Schematic view of the laminate jar containing deionized (DI) water along with the modeled domains.

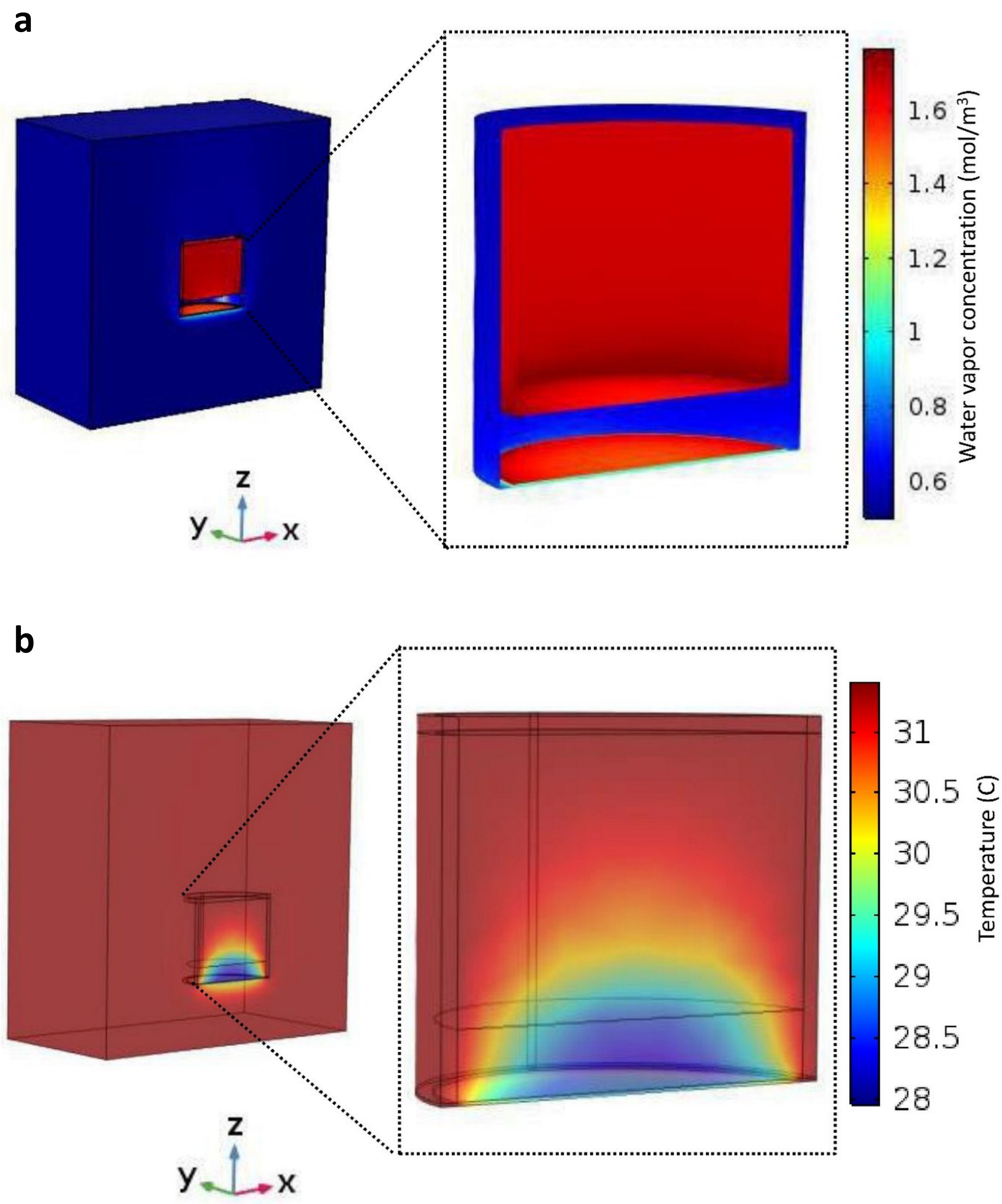

Fig. S2. Distribution of water vapor concentration (a) and temperature (b) for laminate jar drying simulation after 252 min

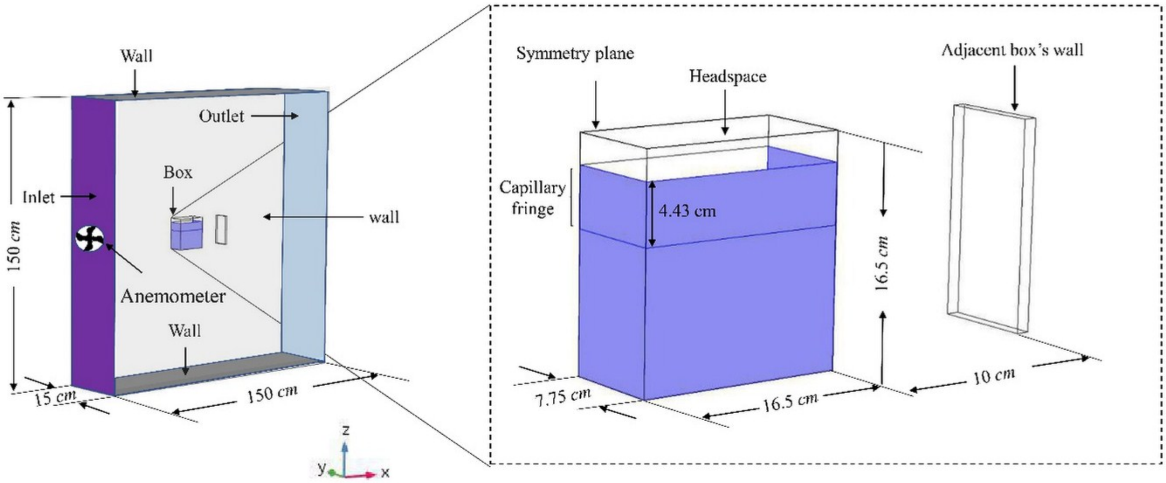

Fig. S3. Schematic view of the laminate box that contained DI water and the modeled domains. The capillary fringe was 4.43 cm in height.

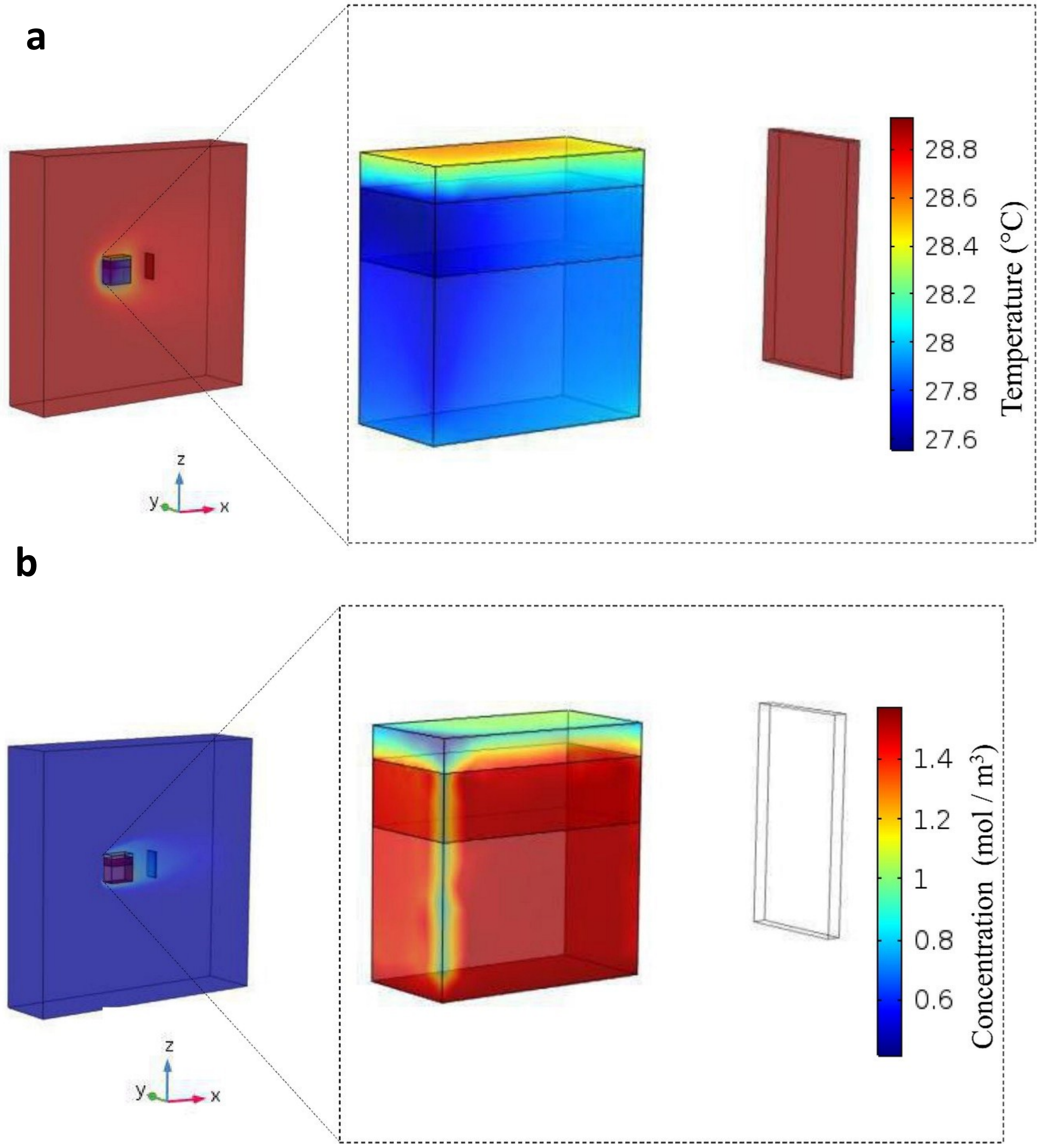

Fig. S4. Distribution of temperature (a) and water vapor concentration (b) for the laminate box drying simulation after 252 min.

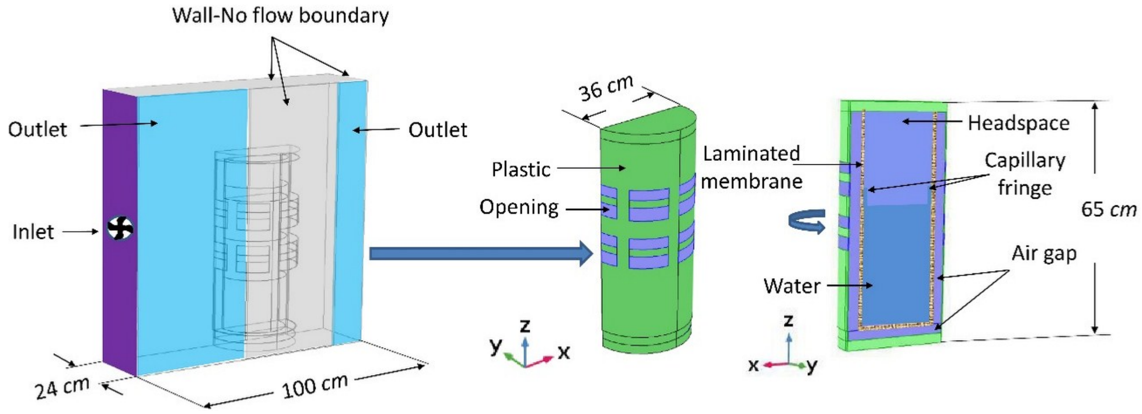

Fig. S5. Schematic of the laminated-lined 40 L toilet and the modeled domains. The drying experiment was conducted at the controlled experimental conditions (capillary fringe = 4.43 cm).

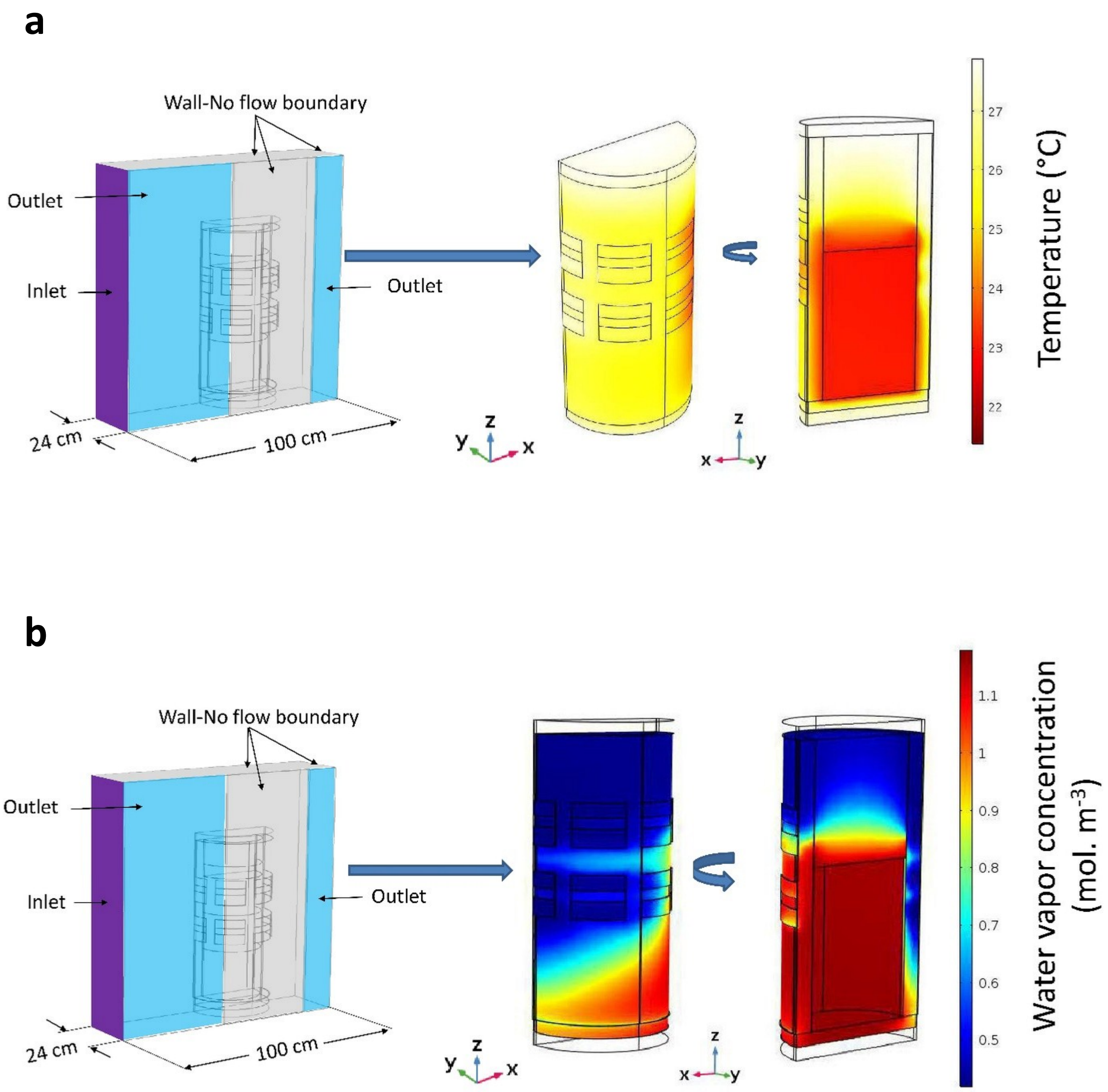

Fig. S6. Distribution of temperature (a) and water vapor concentration (b) for drying simulation of the laminated-lined 40L toilet after 252 min.

a

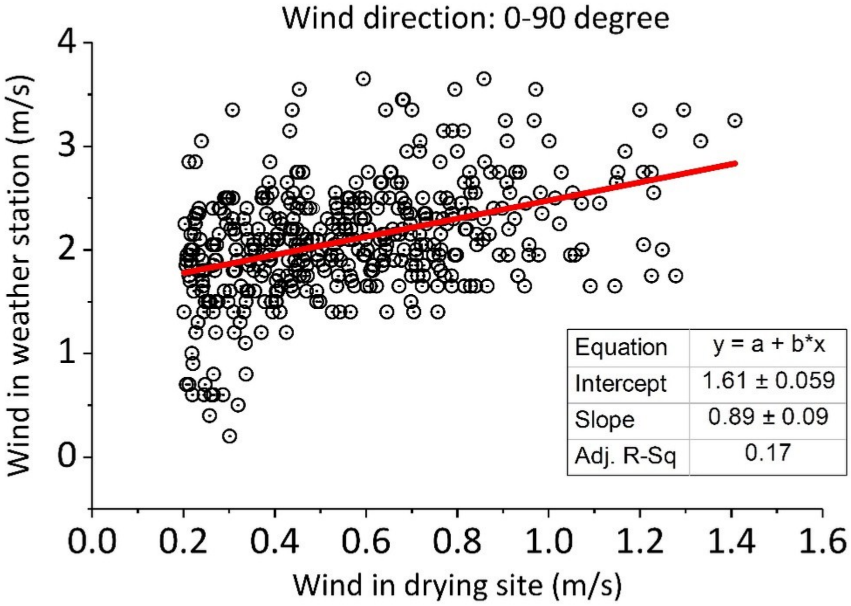

b

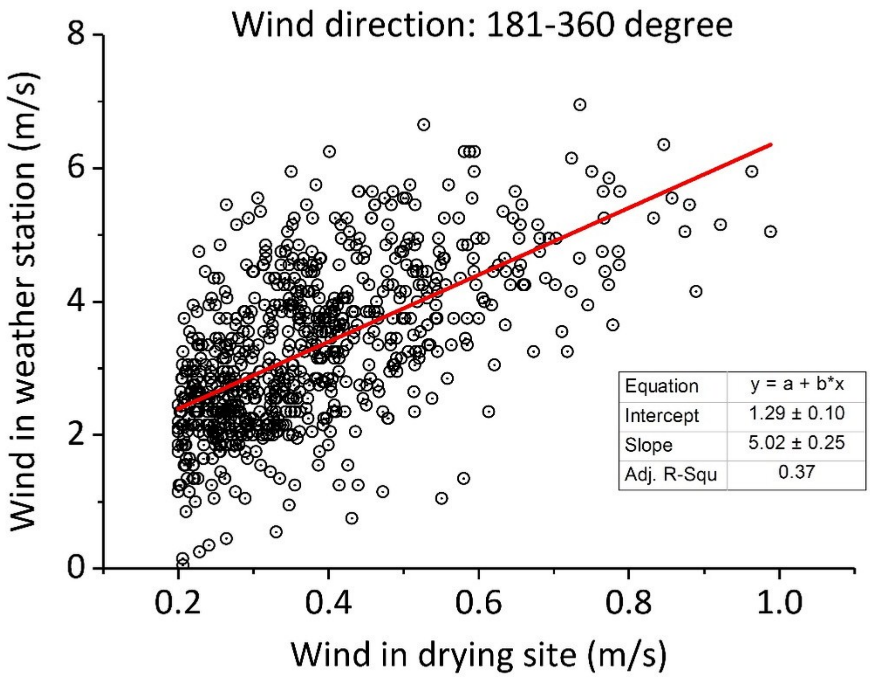

Fig. S7 Correlations developed between wind measured at the drying site and wind recorded at the weather station for high drying rate simulation (a) and low drying rate simulation (b).

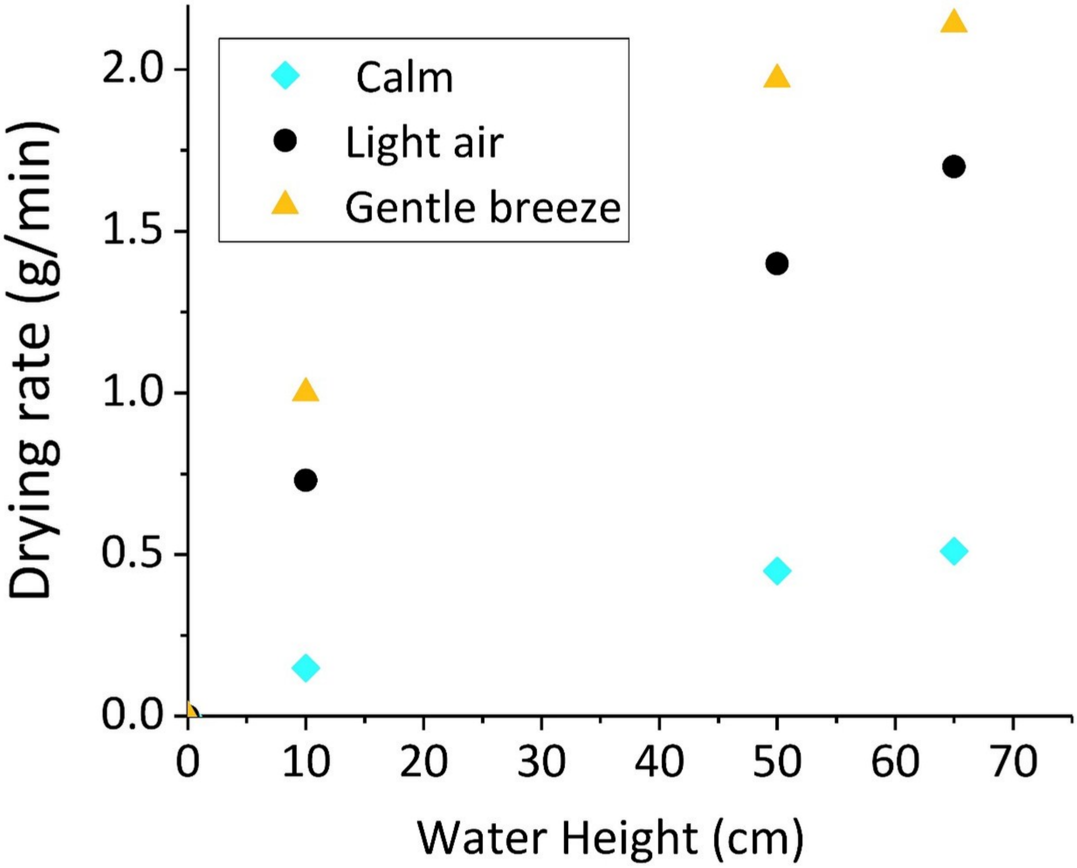

Fig. S8. Drying rate versus water height inside the laminated-lined 40 L drum for three wind speeds used in filling time estimations: calm (<0.1 m/s), light air (1.67 m/s) and gentle breeze (3.4 m/s) for Assab, Eritrea. Drying rates for filling time calculations were linearly interpolated between modeled drying rates plotted here. Similar figures created for the eight other locations shown in Fig. 8 of the manuscript.

References

1 Department of Fire Protection Engineering, University of Maryland College Park, http://www.firebid.umd.edu/material-database.php, (accessed 5/1 2019).

2 Polytetrafluoroethylene properties, https://www.bearingworks.com/uploaded-assets/pdfs/retainers/ptfe-datasheet.pdf, (accessed 5/1 2019).

3 Engineering ToolBox, https://www.engineeringtoolbox.com/, (accessed 5/5 2019).

4 SUBHASIS DAS, *International J. of Management and Applied Science,* 2016, **2**, 57-61.